RSC Advances

ROYAL SOCIETY OF CHEMISTRY

www.rsc.org/advances

A High Performance Ceria-based Solid Oxide Fuel Cell Operating on Underground Coal Gasification Gas

Jie Xiong[*a], Chengran Jiao[b], Minfang Han[c], Wentao Yi[a], Jie Ma[a], Chunyan Yan[a]

([a] *College of Chemistry, Chemical Engineering and Material Science, Zaozhuang University, Zaozhuang* 277160, *Shandong, China*;

[b] *School of Mechanical and Electronic Engineering, Zaozhuang University, Zaozhuang* 277160, *Shandong, China*;

[c] *Department of Thermal Engineering, Tsinghua University, Beijing* 100084, *Beijing, China*)

Abstract

This paper investigates the equilibrium species and theoretical electromotive forces (EMF) of cell fed with 3% H_2O humidified simulated underground coal gasification (UCG) gas, and the performance of anode-supported NiO-$Gd_{0.1}Ce_{0.9}O_{2-\delta}$ (GDC)||GDC||$Ba_{0.9}Co_{0.7}Fe_{0.2}Nb_{0.1}O_{3-\delta}$ ($B_{0.9}$CFN) cell operated on the UCG gas. Results show that EMF values are always above 1.05 V, and the UCG gas fed cell exhibits maximum power densities of 0.151, 0.299, 0.537 and 0.729 $W \cdot cm^{-2}$ at 500, 550, 600 and 650 ^oC, respectively, slightly inferior to that of hydrogen fed cell of 0.330, 0.544, 0.765 and 0.936 $W \cdot cm^{-2}$, respectively, as a result of sluggish reaction kinetics of UCG gas at the anode. However, the synergy between slow anode reaction kinetics and sufficient and fast migration of oxygen ions to the anode attributing to the using of GDC electrolyte and $B_{0.9}$CFN cathode suppresses carbon deposition at intermediate temperatures. Only slight current density decrease ranged from 0.2959 to 0.2790 $A \cdot cm^{-2}$ is observed during the 480 h of durability testing under constant 0.7 V output voltage at 600 ^oC for the UCG gas fed cell. And subsequent

[*] **Corresponding author.** Tel.: +86 632 3786735; fax: +86 632 3786735.
Email address: cumtbxiongjie@163.com (J. Xiong).
Add.: College of Chemistry Chemical Engineering and Material Science, Zaozhuang University, Shandong 277160, P. R. China.

SEM inspection of the tested cell indicates no measurable carbon deposition on the anode surface, thereby demonstrating that UCG gas is a promising fuel for utilization in SOFCs.

Key Words: Solid oxide fuel cell; underground coal gasification; hydrocarbons; thermodynamic equilibrium; carbon deposition

1. Introduction

Many investigations have been carried out on hydrocarbons-fuelled solid oxide fuel cells (SOFCs) because hydrocarbon fuels are readily available and cost effective [1-5]. However, nowadays nearly all SOFC systems designed for operation on hydrocarbon fuels had to convert hydrocarbons into a mixture of hydrogen and carbon monoxide by steam reforming to avoid cracking of hydrocarbons and deposition of carbon at the anode. And an S/C (the molar ratio of steam to carbon) of greater than 2 is usually used to prevent deposition of carbon, which results in decreases in the cell voltage and system efficiency and possible degradation of the anode due to Ni oxidation under condition of high fuel depletion [2,6,7]. Therefore, the development of direct hydrocarbons-fuelled SOFCs without a complex fuel processing system, i.e. an external reformer, is important to SOFC research.

Recently, some successful operation of SOFCs running directly on various hydrocarbons (e.g., natural gas, methanol, gasoline, diesel, octane, etc.) has been reported [1,2,8-10], and these study employed either Ru-, Pt-, Cu-based cermets or perovskite oxides as anodes to resist carbon deposition. Although these approaches are promising, the electrical conductivity and electro-catalytic activity for Cu-based cermets and perovskite oxides are a concern [11-14]. Besides, noble metals such as Pt, Pd and Ru are too expensive to be used in large-scale

commercial application.

As reported Ni is a good catalyst for hydrocarbon cracking reaction [14-17], thereby Ni-based cermets could be a desirable alternative for hydrocarbons internal reforming reaction as long as the cracking carbon particle can be oxidized by O^{2-} immediately. For example, Koh et al [18] found SOFCs on 3 vol.% H_2O humidified methane by employing a Ni-YSZ anode could operate without carbon deposition at 750 ^oC, when the cell current density was higher than 100 $mA \cdot cm^{-2}$. However, carbon deposition was favored dynamically when the cell ran at a lower current density. Thus, it is evident that high current density allows sufficient O^{2-} supply to combine hydrocarbon and thereby avoiding carbon deposition successfully. So in that sense, it'll be better to substitute gadolinia-doped ceria (GDC) for YSZ, because the ionic conductivity of GDC was reported from 1.01×10^{-2} to 2.53×10^{-2} $S \cdot cm^{-1}$ at 600 ^oC, which is two orders of magnitude higher than that of the YSZ electrolyte (approximately 10^{-4} $S \cdot cm^{-1}$) at the same temperature [19,20]. Thus GDC can provide much higher oxygen ion conductivity for the anodes and enhance the oxidation rate of cracking carbon. And another advantage for GDC is that the doped-ceria material has an ability for continuous carbon cleaning due to its oxygen storage/release capacity [15,21].

So far, the influence of various hydrocarbons on the performance and durability of SOFCs has been reported and the results are available in the literature. Nevertheless, the study of SOFC fed with underground coal gasification (UCG) gas, a widely used hydrocarbon in China, Australia and India, is rarely reported [22,23]. UCG is a clean coal technology with in situ gasification which largely eliminates the mining problem and the ash disposal problem while offering the possibility of economical exploitation of low rank coal, even offers an attractive option of utilizing

unmineable coal [22-24]. And SOFC can convert chemical energy in the fuel directly to electricity with fuel flexibility, high efficiency, and low emissions of greenhouse gas such as CO_2 and environmental pollutants like NO_x [25-27]. If researchers could couple UCG with an SOFC to generate electrical power directly, it will be a both environmentally friendly and high efficiency power-generating approach. The aim of this work was to demonstrate the possibilities, both in theory and practice, of operation on UCG gas fuels using a state-of-the-art solid oxide fuel cell with Ni/GDC cermet anode and a newly developed A-site deficient $Ba_{0.9}Co_{0.7}Fe_{0.2}Nb_{0.1}O_{3-\delta}$ cathode.

2. Experimental section

A SOFC is essentially an oxygen concentration cell where an electromotive force (EMF) is produced due to the electrochemical potential gradient of oxygen between the anode and the cathode of the cell. The EMF for SOFC can be described by the following Nernst Eq. (1), given that the electrolyte is a pure ionic conductor [28]:

$$E = \frac{RT}{4F} ln \frac{P_{O_2}^{'}}{P_{O_2}^{''}} \qquad (1)$$

where R is the gas constant, T is the absolute temperature, F is the Faraday constant, and $P_{O_2}^{'}$ and $P_{O_2}^{''}$ are the oxygen partial pressures at the cathode and the anode, respectively.

The cathode is exposed to ambient air in a fuel cell, so $P_{O_2}^{'}$ is equal to 0.21 atmospheric pressure. While $P_{O_2}^{''}$, oxygen partial pressure in the fuel, is determined thermodynamically. The equilibrium composition of a fuel mixture is calculated by means of the Gibbs free energy minimization method [29]. The EMFs for SOFCs running on 3% H_2O-humidified H_2 or simulated underground coal gasification (UCG) gas were calculated according to Eq. (1).

To prepare anodes, $Gd_{0.1}Ce_{0.9}O_{2-\delta}$ (GDC) and NiO powders in a weight ratio of 1:1 were mixed thoroughly, followed by additions of ethanol and butanone solvent, polyvinyl butyral binder, dibutyl phthalate plasticizer, castor oil dispersant and graphite pore former in appropriate proportions. After ball milling for 24 h, the slurry was tape cast. Green tapes, approximately 0.5 mm thick were obtained, and then pellets with a diameter of 20 mm were punched from these tapes. After burning out binder at 1000 ^{o}C in air for 2 h, disks of porous NiO/GDC anode substrates were obtained. An electrolyte suspension comprising of GDC, ethylcellulose and terpineol was ball milled for 24 h, and then this electrolyte slurry was coated on the presintered anode substrates. Subsequently, the pellets consisting of anode substrate coated with the GDC electrolyte slurry were co-fired at 1350 ^{o}C for 5 h in air to produce the anode-supported half-cell. Then A-site deficient $Ba_{0.9}Co_{0.7}Fe_{0.2}Nb_{0.1}O_{3-\delta}$ ($B_{0.9}$CFN) cathode paste was screen printed on the other surface of the GDC electrolyte as reported in a previous study [30], followed by sintering at 1000 ^{o}C for 2 h to get the single cells, and the effective area of the cathode was 0.28 cm^2.

The final anode-supported NiO-GDC||GDC||$B_{0.9}$CFN fuel cell was then sealed on an alumina tube with a ceramic sealant (CERAMABOND 552, USA). After sealing, cell performances including I-V characterizations and long term stability were evaluated with an Arbin multi-channel instrument (BT2000, USA) at various temperatures (500~650 ^{o}C) in H_2 and simulated UCG gas with 3 vol.% H_2O at a flow rate of 80 mL·min^{-1} on the anode side and stationary air on the cathode side. The electrochemical impedance of the cells was investigated under open circuit conditions using an electrochemical workstation (IM6, ZAHNER, Germany) in the frequency range of 0.01 Hz to 4 MHz with 10 mV as the excitation ac amplitude. And the microstructures of single cell before testing and Ni/GDC anode after cell performance stability test

were observed by a field emission scanning electron microscope (JSM-7800F, JEOL, Japan) with an energy dispersive X-ray detector (X-Max, Oxford, England).

3. Results and discussion

The composition of the simulated UCG gas is listed in Table 1.

The equilibrium concentration of chemical species in cell fed with 3% H_2O humidified simulated UCG gas are presented as a function of temperature between 400 and 900 ^oC in Fig. 1, assuming that various chemical species reach complete thermodynamic equilibrium. The molar fraction labeled in figure is the concentration of chemical species in the total equilibrium products including solid graphite $C_{(s)}$. The derived equilibrium products as shown in Fig. 1 indicates that no graphite thermodynamically forms below 450 ^oC, and the graphite deposition above 450 ^oC progressively intensifies with increasing temperature, and the concentration of decomposed carbon at all temperature is less than ten percent. The amounts of H_2 and CO increase steadily with increasing temperature, while CH_4 and H_2O follow a reverse pattern. The CO_2 and H_2O species will be helpful in inhibiting carbon deposition at anode via CO_2 reforming and steam reforming.

Fig. 2 shows the temperature dependence of the equilibrium oxygen partial pressures at anode and calculated EMF of a SOFC running on humidified H_2 and simulated UCG gas. The oxygen partial pressure at anode in the simulated UCG gas increases with temperature from 10^{-30} kPa at 400 ^oC to 10^{-19} kPa at 900 ^oC, which is higher than that in the equilibrium systems of hydrogen below 770 ^oC, and lower than that of hydrogen above 770 ^oC. However, a high oxygen partial pressure at the anode causes a decrease in EMF according to Eq. (1). As can be seen in Fig. 2, the lower equilibrium oxygen partial pressure from hydrogen gives rise to the higher EMF at

temperatures below 770 ^{o}C, while the UCG gas achieves the higher EMF as a result of the lower oxygen partial pressure when temperature is higher than 770 ^{o}C. Moreover, the EMF for simulated UCG gas increases monotonically with increasing temperature, just opposite of the trend shown for hydrogen, and EMF values at all temperatures were above 1.05 V. The high EMF indicates operating SOFCs with UCG gas is feasible.

A cross sectional image of the NiO-GDC||GDC||$B_{0.9}$CFN single cell before testing is exhibited in Fig. 3. It can be observed that the mutual components of SOFC contact tightly, without de-lamination, crack, or obvious defects, and the interface is smooth and regular. The GDC electrolyte is dense with a thickness of 13 μm. The $B_{0.9}$CFN cathode layer has porous structure and a thickness of approximately 25 μm. However, the porosity in the anode is slightly lower, which could be improved naturally after the reduction of NiO particle in anode. The well adhesion between the dense electrolyte and porous electrodes as displayed could extend the spatial structure, lengthen the triple phase boundaries, and thus increase the active sites substantially as well as ensure good electrochemical performance and durability of cell.

Fig. 4a depicts the cell impedance spectra for 3% H_2O humidified H_2 and simulated UCG gas at different temperatures under open circuit condition. The high frequency intercept represents ohmic resistance R_o of the cell, and the differences of ohmic resistance between H_2 and simulated UCG gas as the fuel were almost negligible, indicating the bulk resistance of cells in the two fuels remains to be same. But the polarization resistance R_p (i.e. the difference between the intercepts of the impedance arc on the real axis) of cell with simulated UCG gas were relatively higher than that of cell with H_2 fuel at all temperature. Moreover, the differences of R_p values of cells with H_2 and simulated UCG gas decreased with increasing temperature, and the polarization resistance of cells

with the two fuels at 650 ^{o}C were relatively close to each other, implying the UCG gas fed cell would produce high power output at intermediate temperature. From the polarization resistances of symmetrical cell of $B_{0.9}$CFN electrodes measured on GDC electrolyte with a configuration of $B_{0.9}$CFN||GDC||$B_{0.9}$CFN in 3% H_2O humidified H_2 and simulated UCG gas at 500~650 ^{o}C under open circuit conditions shown in Fig. 4b, the activation energies can be determined to be 0.75 and 0.95 eV for hydrogen and UCG gas, respectively. The higher activation energy for UCG gas results in slow kinetics at low temperatures that likely caused the relatively decreased maximum powder density (MPD) as shown in Fig. 5. However, the activation energy for UCG gas is much lower than those of other hydrocarbon fuels. For example, the activation energy for 3% H_2O humidified CH_4 was reported to be 1.18~1.31 eV [31], and the activation energy for C_4H_{10} was as high as 202 kJ·mol^{-1} [32], i.e. 2.09 eV. Thus, UCG gas fuel is expected to have higher MPD than other hydrocarbons, especially at intermediate temperature.

The current-voltage and current-power characterization of cells on humidified H_2 and simulated UCG gas at temperatures ranging from 500 to 650 ^{o}C is presented in Fig. 5. As expected, the performance was enhanced with increasing temperature. The cell with hydrogen as fuel always gave the higher power, with maximum power densities of 0.330, 0.544, 0.765 and 0.936 W·cm^{-2} at 500, 550, 600 and 650 ^{o}C, respectively. And the UCG gas fueled cell exhibited the maximum powder densities of 0.151, 0.299, 0.537 and 0.729 W·cm^{-2}, respectively, at 500, 550, 600 and 650^{o}C, which are little higher than that of methanol fueled SOFC [9], and at least twice the maximum power density of that of methane fueled SOFCs [33,34]. For clarity, the measured open circuit voltage (OCV) values are listed in Table 2, including the calculated EMF values in parentheses. The trend of experimental OCV values and the calculated EMF values with

temperature is the same. Although the experimental OCV values are less than calculated EMF ones, presumably indicating the existence of electronic conductivity in the GDC electrolyte under reducing atmosphere from the partial reduction of Ce^{4+} to Ce^{3+}, the measured OCV values of H_2 and simulated UCG gas fed cells appear to be equally matched. So it is reasonable to draw the conclusion that UCG gas shows excellent prospects as a fuel for ceria-based SOFCs at intermediate temperature.

The performance stability of the cells was also investigated. The current density at a constant cell voltage of 0.7 V at 600 ^{o}C with H_2 and simulated UCG gas as a function of time is shown in Fig. 6. No measurable performance loss was observed in the case of hydrogen fueled cell, implying superior chemical stability of $B_{0.9}$CFN, steady electric characteristics of electrodes, and strong bonding between electrolyte and electrodes, as shown in Fig. 3. For the cell operating on UCG gas, a slight current density decrease ranged from 0.2959 to 0.2790 A·cm^{-2} was observed during the 480 h of testing, and subsequent cross-sectional SEM inspection (Fig. 7) of the tested cell indicated no measurable carbon deposition on the anode surface. Furtherly, the EDS results for the NiO-GDC anode after performance stability testing with simulated UCG gas are displayed in Fig. 8, and little C peak was found. Therefore, it can be concluded that the ceria-based anode supported SOFC with $B_{0.9}$CFN cathode can effectively inhibit or remove carbon species when using UCG gas as fuel. The cell running on UCG gas exhibited a reliable durability due to the much higher current density obtained at 0.7 V than the critical current density of 0.100 A·cm^{-2} for carbon deposition mentioned by Koh et al [18] using 3 vol.% H_2O humidified methane fuel gas by employing a Ni-YSZ anode at 750 ^{o}C.

Since fuel gas at a constant rate of 80 mL·min^{-1}, the theoretical carbon deposition can be

calculated on the basis of ideal gas state equation and equilibrium compositions of UCG gas showed in Fig. 1, and the theoretical carbon deposition of cell running on humidified simulated UCG gas at 600 ^{o}C is 0.006812mol·h^{-1} (i.e., 0.08174g·h^{-1} carbon). However, the coking result of cell running on simulated UCG gas was not as bad as predicted. There may be two reasons for the better than predicted long-term stability. On one hand, the slow kinetics at 600 ^{o}C causes less pyrolysis of methane species in the UCG gas, resulting in less coke formation, since thermodynamic equilibrium analysis assumes that all chemical species reach complete thermodynamic equilibrium at anode side, yet the equilibration kinetics factor is not fully considered. On the other hand, the relatively sufficient O^{2-} supply to react with deposited carbon particles due to fast migration of oxygen ions contributes to inhibition of carbon deposition at low operating temperatures. We assume that A-site deficient $B_{0.9}$CFN is responsible for the adequate O^{2-} transport from the cathode to the anode, because additional oxygen vacancies created from A-site deficiencies are beneficial to the oxygen reduction reaction and facilitate oxygen ion diffusion within the oxide bulk as our previous study [30,35,36], along with others [37,38]. Meanwhile, the GDC electrolyte contributes to the fast migration of oxygen ions due to its relatively higher ionic conductivity at intermediate temperatures. So even if some carbon deposits would occur, the oxygen species from GDC can promote their removal, similar to the effects of ceria-based materials mentioned in other literatures [39,40]. The Ni-GDC||GDC||$B_{0.9}$CFN cell fed with UCG gas demonstrated an excellent stability against coke formation, maintaining a relatively stable current density, suggesting that the UCG gas could be a potential hydrocarbon fuel for SOFCs.

4. Conclusions

The equilibrium compositions of fuel in cell fed with 3% H_2O humidified simulated UCG gas were calculated in the temperature range between 400 and 900 ^oC based on thermochemical calculations using Gibbs free energy minimization method, assuming that various chemical species reached complete thermodynamic equilibrium. Based on these equilibrium compositions, the EMFs for SOFCs running on H_2 and simulated UCG gas were calculated. Afterwards these two fuels were supplied to ceria-based electrolyte single cells, and a systematic study was conducted. Compared to calculated EMFs assuming pure ionic conducting electrolyte is adopted, the measured OCVs of the cells were lower indicating some electronic conduction in the GDC electrolyte under the temperatures and oxygen pressures employed in this study. Besides, the UCG gas fed cell demonstrated exceptional electrochemical performance, only slightly inferior to that of hydrogen fed cell, and comparatively stable long-term stability. SEM inspection of a cell after 480 h of operation in UCG gas at 600 ^oC at 0.7 V showed that the anode itself remained free of any carbon deposits. This work suggests that the UCG gas has an intriguing future for direct utilization in SOFCs, and affords the simplicity of not having to reform the fuel with an expensive external reformer. Such a fuel would be ideal for industrial integrated coal gasification fuel cell system (IGFC).

Acknowledgements

Financial supports from MOST of China (2012CB215404) and the NSFC of China (51261120378) are greatly appreciated.

References

[1] Z. L. Zhan and S. A. Barnett, *Science*, 2005, **308**, 844.

[2] M. L. Faro and A. S. Arico, *Int. J. Hydrogen Energy*, 2013, **38**, 14773.

[3] T. J. Lee and K. Kendall, *J. Power Sources*, 2008, **181**, 195.

[4] T. M. Gur, M. Homel and A. V. Virkar, *J. Power Sources*, 2010, **195**, 1085.

[5] Y. M. Park and H. Kim, *Int. J. Hydrogen Energy*, 2014, **39**, 16513.

[6] P. Hofmann, K. D. Panopoulos, L. E. Fryda, A. Schweiger, J. P. Ouweltjes and J. Karl, *Int. J. Hydrogen Energy*, 2008, **33**, 2834.

[7] J. G. Lee, C. M. Lee, M. Park and Y. G. Shul, *RSC Adv.*, 2013, **3**, 11816.

[8] J. Liu and S. A. Barnett, *Solid State Ionics*, 2003, **158**, 11.

[9] M. F. Liu, R. R. Peng, D. H. Dong, J. F. Gao, X. Q. Liu and G. Y. Meng, *J. Power Sources*, 2008, **185**, 188.

[10] H. Q. Li, Y. Tian, Z. M. Wang, F. C. Qie and Y. D. Li, *RSC Adv.*, 2012, **2**, 3857.

[11] Z. B. Yang, Y. Chen, C. Jin, G. L. Xiao, M. F. Han and F. L. Chen, *RSC Adv.*, 2015, **5**, 2702.

[12] Y. Q. Li, X. B. Zhu, Z. Lu, Z. H. Wang, W. Jiang, X. Q. Huang and W. H. Su, *Int. J. Hydrogen Energy*, 2014, **39**, 7980.

[13] P. Zhang, Y. H. Huang, J. G. Cheng, Z. Q. Mao and J. B. Goodenough, *J. Power Sources*, 2011, **196**, 1738.

[14] S. D. Song, M. F. Han, J. Q. Zhang and H. Fan, *J. Power Sources*, 2013, **233**, 62.

[15] M. J. Escudero, I. Gómez de Parada, A. Fuerte and J. L. Serrano, *J. Power Sources*, 2014, **253**, 64.

[16] S. E. Evans, O. J. Good, J. Z. Staniforth, R. M. Ormerod and R. J. Darton, *RSC Adv.*, 2014, **4**, 30816.

[17] C. W. Sun and U. Stimming, *J. Power Sources*, 2007, **171**, 247.

[18] J. H. Koh, Y. S. Yoo, J. W. Park and H. C. Lim, *Solid State Ionics*, 2002, **149**, 157.

[19] B. C. H. Steele, *Solid State Ionics*, 2000, **129**, 95.

[20] D. J. Seo, K. O. Ryu, S. B. Park, K. Y. Kim and R. H. Song, *Mater. Res. Bull.*, 2006, **41**, 359.

[21] M. J. Beier, T. W. Hansen and J. D. Grunwaldt, *J. Catal.*, 2009, **266**, 320.

[22] V. Prabu and S. Jayanti, *Appl. Energy*, 2012, **94**, 406.

[23] V. Prabu and S. Jayanti, *Int. J. Hydrogen Energy*, 2012, **37**, 1677.

[24] A. W. Bhutto, A. A. Bazmi and G. Zahedi, *Prog. Energy Combust. Sci.*, 2013, **39**, 189.

[25] P. Arunkumar, S. Preethi and K. S. Babu, *RSC Adv.*, 2014, **4**, 44367.

[26] F. Wang, W. Wang, J. F. Qu, Y. J. Zhong, M. O. Tade and Z. P. Shao, *Environ. Sci. Technol.,* 2014, **48**, 124277.

[27] S. M. Jamil, M. H. D. Othman, M. A. Rahman, J. Jaafar, A. F. Ismail and M. A. Mohamed, *RSC Adv.*, 2015, **5**, 58154.

[28] T. Kudo and H. Obayashi, *J. Electrochem. Soc.*, 1976, **123**, 415.

[29] K. Sasaki and Y. Teraoka, *J. Electrochem. Soc.*, 2003, **150**, A878.

[30] Z. Liu, L. Z. Cheng and M. F. Han, *J. Power Sources*, 2011, **196**, 868.

[31] H. Lv, D. J. Yang, X. M. Pan, J. S. Zheng, C. M. Zhang, W. Zhou, J. X. Ma and K. A. Hu, *Mater. Res. Bull.*, 2009, **44**, 1244.

[32] C. Lu, W. L. Worrell, R. J. Gorte and J. M. Vohs, *J. Electrochem. Soc.*, 2003, **150**, A354.

[33] Y. B. Lin, Z. L. Zhan, J. Liu and S. A. Barnett, *Solid State Ionics*, 2005, **176**, 1827.

[34] B. Huang, X. F. Ye, S. R. Wang, H. W. Nie, J. Shi, Q. Hu, J. Q. Qian, X. F. Sun and T. L.Wen, *J. Power Sources*, 2006, **162**, 1172.

[35] Z. B. Yang, C. Jin, C. H. Yang, M. F. Han and F. L. Chen, *Int. J. Hydrogen Energy*, 2011, **36**, 11572.

[36] Z. B. Yang, C. H. Yang, C. Jin, M. F. Han and F. L. Chen, *Electrochem. Commun.*, 2011, **13**, 882.

[37] H. L. Zhao, Y. F. Cheng, N. S. Xu, Y. Li, F. S. Li, W. Z. Ding and X. G. Lu, *Solid State Ionics*, 2010, **181**, 354.

[38] F. C. Wang, D. J. Chen and Z. P. Shao, *Electrochim. Acta*, 2013, **103**, 23.

[39] Y. Li, X. X. Wang, C. Xie and C. S. Song. *Appl. Catal. A: Gen.*, 2009, **357**, 213.

[40] Z. M. Wang, Y. Li and J. W. Schwank, *J. Power Sources*, 2014, **248**, 239.

Figure captions

Fig. 1. Calculated equilibrium product distribution as a function of temperature for 3% H_2O humidified simulated UCG gas.

Fig. 2. Variation of equilibrium oxygen partial pressure at anode (hollow symbols) and EMF (solid symbols) with temperature for cells fuelled by 3% H_2O humidified H_2 and simulated UCG gas.

Fig. 3. A cross-sectional view of the NiO-GDC||GDC||$B_{0.9}$CFN single cell before testing.

Fig. 4. (a) Cell impedance and (b) electrode polarization resistance of symmetrical cells as a function of operating temperature.

Fig. 5. Voltage and power density versus current density curves for cells on (a) 3% H_2O humidified H_2 and (b) simulated UCG gas at various temperatures.

Fig. 6. Time-dependent history of current density at 0.7 V for cells fed with 3% H_2O humidified H_2 and simulated UCG gas at 600 ^oC.

Fig. 7. Cross-sectional SEM micrographs of Ni/GDC anodes exposed on 3% H_2O humidified simulated UCG gas after cell performance stability test at 600 ^oC.

Fig. 8. EDX results for the NiO-GDC anode after operation with simulated UCG gas (3% H_2O) at 600 ^oC for 480 h.

Table captions

Table 1. The composition of simulated UCG gas at room temperature.

Table 2. Experimental open circuit voltage and thermochemically calculated EMF (in parentheses) at various temperatures.

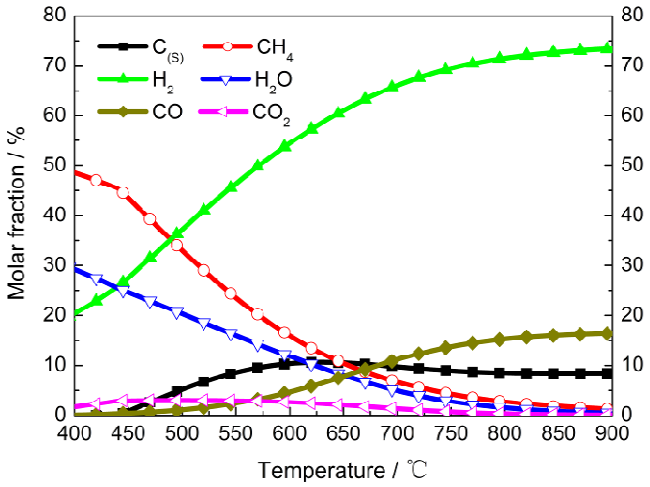

Fig. 1.

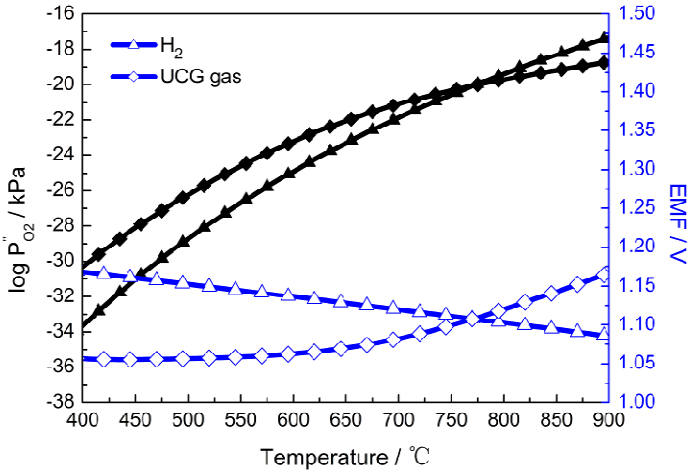

Fig. 2.

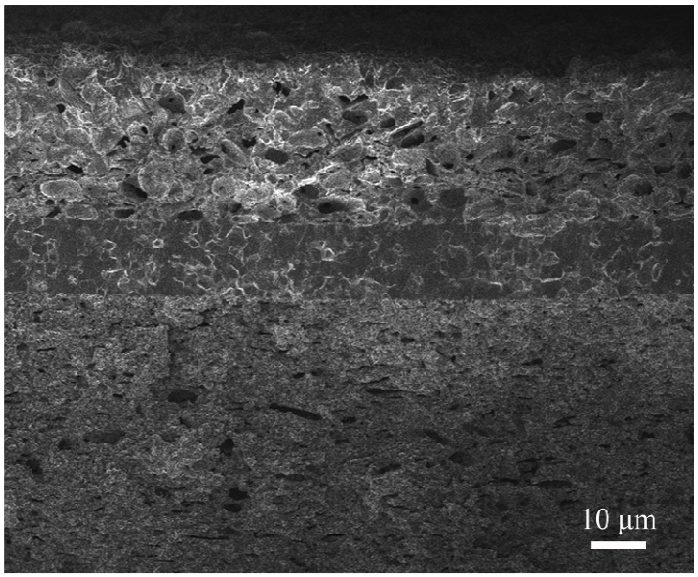

Fig. 3.

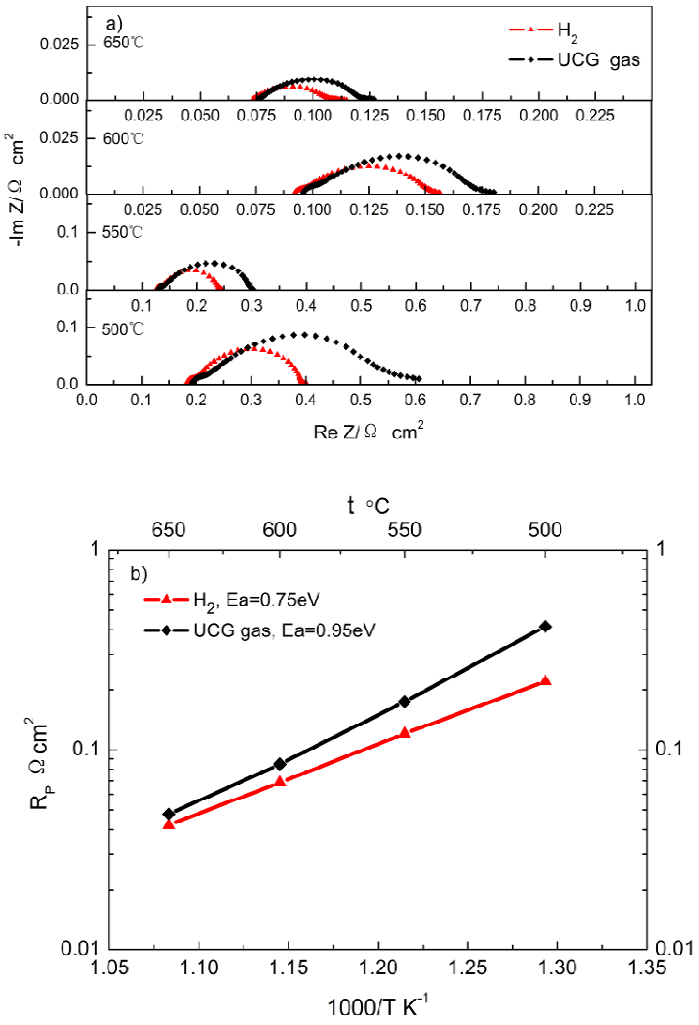

Fig. 4.

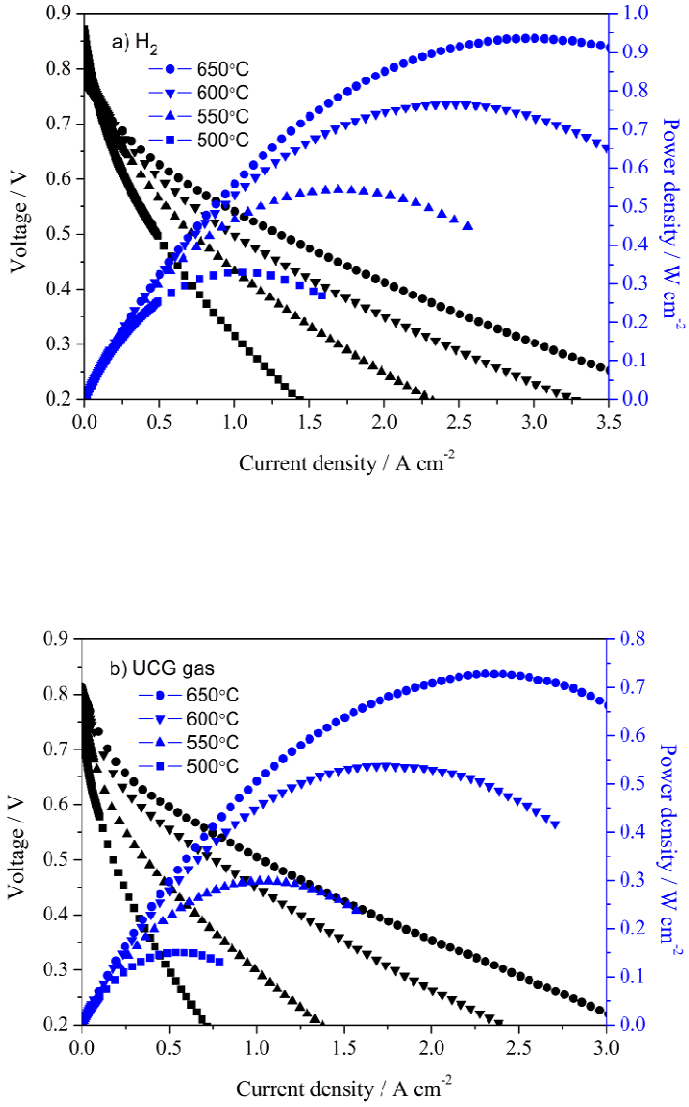

Fig. 5.

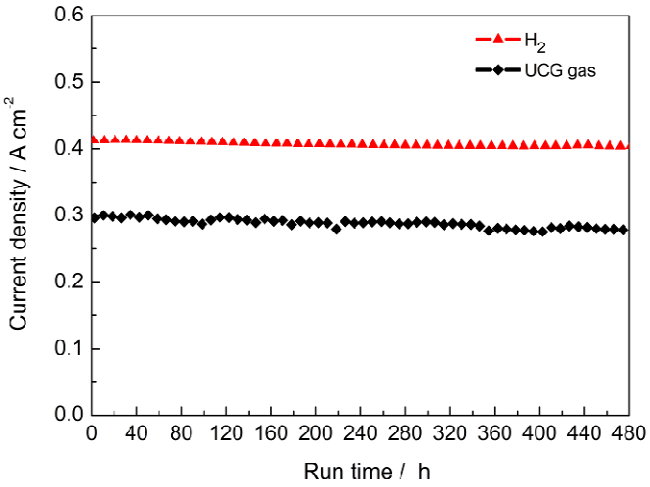

Fig. 6.

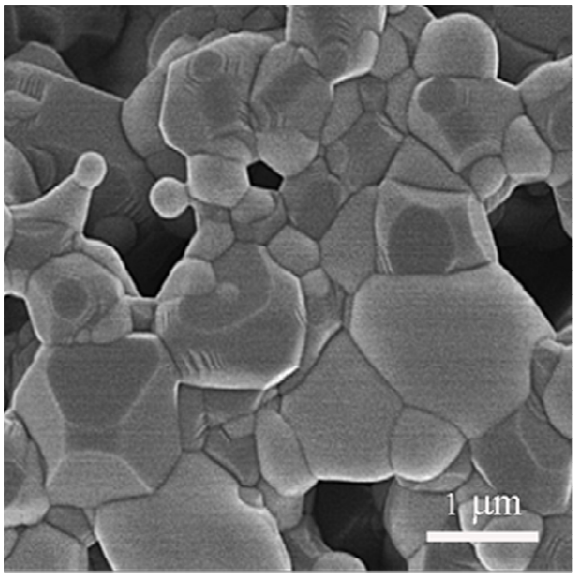

Fig. 7.

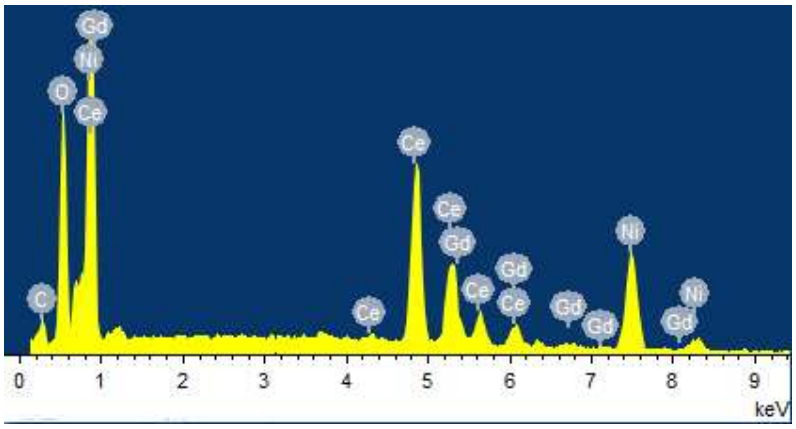

Fig. 8.

Table 1.

Constituents	H_2	CO	CH_4
Volumetric percentages (%)	66	19	15

Table 2.

Temperature / ^{o}C	Open Circuit Voltage (Calculated EMF)/V	
	H_2	UCG gas
500	0.872 (1.152)	0.779 (1.057)
550	0.835 (1.144)	0.786 (1.059)
600	0.805 (1.136)	0.808 (1.063)
650	0.777 (1.128)	0.814 (1.070)